Dalton Transactions

RSC Publishing

PAPER

View Article Online
View Journal | View Issue

Cite this: *Dalton Trans.*, 2013, **42**, 5661

[Ru(bpy)$_2$dppz-idzo]$^{2+}$: a colorimetric molecular "light switch" and powerful stabilizer for G-quadruplex DNA†

Jun-Liang Yao, Xing Gao, Wenliang Sun, Shuo Shi* and Tian-Ming Yao*

Received 5th November 2012,
Accepted 22nd January 2013

DOI: 10.1039/c3dt32640c

www.rsc.org/dalton

A new ruthenium complex, [Ru(bpy)$_2$dppz-idzo]$^{2+}$ (bpy = 2,2′-bipyridine, dppz-idzo = dipyrido-[3,2-*a*:2′,3′-*c*] phenazine-imidazolone), was synthesized and characterized. The luminescent titrations showed that the Ru-complex exhibited an outstanding "light switch" effect with an emission enhancement factor of about 300 in the presence of G-quadruplex DNA in a K^+ solution. This remarkable "light switch" behavior can even be observed by the naked eye under irradiation with UV light. To get an insight into the "light switch" mechanism, quantum-chemical calculations were performed based on the DFT/TDDFT/PCM method at the B3LYP/6-31G* level. Furthermore, the CD titrations and thermal melting experiments indicated that [Ru(bpy)$_2$dppz-idzo]$^{2+}$ could not only induce the formation of an antiparallel G-quadruplex structure in the absence of monocations, but also has the ability to stabilize the G-quadruplex architecture, implying potential applications in anticancer therapeutics. Both the "light switch" effect and the structure stabilization ability of [Ru(bpy)$_2$dppz-idzo]$^{2+}$ were found to be superior to the well-known DNA molecular "light switch" [Ru(bpy)$_2$dppz]$^{2+}$. Finally, a "sandwich-like" binding model was proposed on the basis of molecular docking simulations.

Introduction

Among a variety of non-canonical DNA structures, the G-quadruplex architectures have attracted intense attention as prospective targets for the chemical intervention of biological functions.[1–3] G-quadruplexes are four-stranded nucleic acid structures containing planar G-quartets stabilized by Hoogsteen hydrogen bondings.[4–6] The structures and stability of G-quadruplexes are quite sensitive to monocations. For instance, Na^+ induces antiparallel quadruplex folding in the telomere sequence d[AGGG(TTAGGG)$_3$] (22AG), while K^+ induces a hybrid-type mixed parallel/antiparallel G-quadruplex structure (Fig. 1).[7–9] The folding pathways of these specific G-quadruplex conformations have also been reported recently.[10]

The first glimpse of a new era for DNA-targeted therapeutics came through the realization that telomeres can form G-quadruplexes.[11,12] Telomeres, a specialized functional nucleoprotein structure located at the ends of eukaryotic chromosomes, play an important role in structural chromosome integrity. Telomeres function to cap and protect chromosome termini from illegitimate recombination, degradation, and end-to-end fusion.[13,14] In humans, telomeres consist of a repetition of the double-stranded DNA sequence (5′-TTAGGG)/(5′-CCCTAA), with the G-rich 3′ region extending beyond the duplex to form a single stranded overhang, called the G-overhang.[15,16] These 3′ overhangs are relatively long (50–210 bases in length) and present on all chromosomal ends.[15,17]

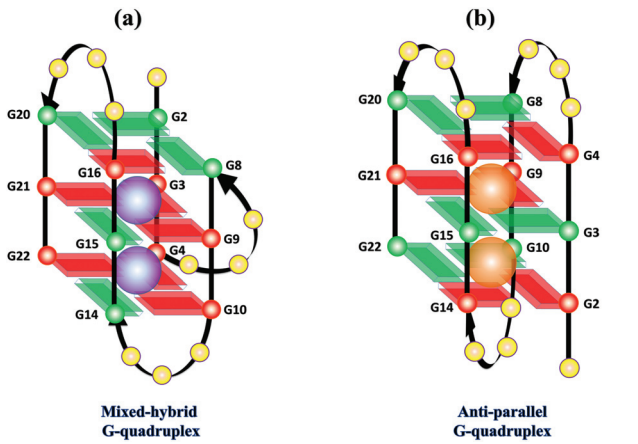

Fig. 1 Structures of intramolecular G-quadruplexes formed from human telomeric DNA sequences in K^+ (a) and Na^+ (b) solutions. The potassium and sodium ions are shown as lavender and orange spheres, respectively.

Department of Chemistry, Tongji University, Shanghai, China.
E-mail: shishuo@tongji.edu.cn, tmyao@tongji.edu.cn; Fax: +86-21-6598-2287; Tel: +86-21-6598-3292

†Electronic supplementary information (ESI) available: absorption titrations and some detailed results of the computational calculations. See DOI: 10.1039/c3dt32640c

Because of the repetition of guanines, the G-overhang is prone to form four-stranded polymorphic G-quadruplex structures. G-quadruplex conformations may be capable of both shortening the telomere and directly causing telomere uncapping, leading to the inhibition of the catalytic lengthening activity of telomerase by disrupting the interaction between the enzyme and its substrate.[18] It has been shown that telomerase is over-expressed in approximately 85% of cancer cells and plays an essential role in their immortalization.[19,20] Numerous observations, notably that inhibiting telomerase activity and/or interfering with the telomere capping function limits tumor cell growth, have given rise to the proposal that telomeres and telomerase are potential targets for cancer chemotherapy.[21–23] Hence, there is great current interest in developing small molecules that bind and stabilize telomeric G-quadruplex structures.[24–26] The biological and therapeutic significance of telomeric G-quadruplexes is well appreciated and continues to be an active field for drug discovery.

In addition, the abundance of G-rich repeats was also found to be linked with nuclease hypersensitive regions within DNA promoter regions of the human genome, suggesting that guanine-rich duplex DNA sequences within promoter regions are involved in modulating gene transcription.[27,28] Although these sequences are usually paired with complimentary DNA strands, during transcription and replication duplex unwinding would expose the single G-rich strand and allow intramolecular folding.[29,30] The therapeutic potential of gene promoter G-quadruplexes has sparked great interest in the design of molecules that can act as G-quadruplex stabilizers.[31–33] In terms of therapeutic targets, the gene promoter regions, with their various sequences, may provide specific scaffolds that are ideal for designing selective ligands.[11] Moreover, recent investigations found that transcribed single-stranded G-rich noncoding RNA sequences, particularly within mRNA, could readily form more stable G-quadruplexes *in vitro* than DNA.[34–36] Further characterization of these RNA quadruplexes could provide the basis for a rational approach towards translational control of gene expression by employing small-molecule ligands. In comparison with DNA, RNAs are inherently single-stranded, distributed more widely in cells and can readily fold into very stable G-quadruplex topologies, indicating that G-rich RNAs may prove to be a class of more attractive therapeutic targets.[37]

It has been reported that a number of metal complexes can also interact strongly and selectively with quadruplex DNA, apart from the purely organic heteroaromatic compounds reported previously.[38–43] In comparison with organic compounds, metal complexes have a very broad range of structural and electronic properties that can be successfully exploited when designing quadruplex DNA binders. The metal center can play a major structural role in organizing ligands in specific geometries and relative orientations for optimal quadruplex interaction. Moreover, the electron density on coordinated aromatic ligands can be reduced by the electron-withdrawing properties of metal centers and consequently, electron-poor systems are expected to exhibit stronger π interactions with G-quartets. Also, some of the electropositive metals can, in principle, be positioned at the center of the guanine quartet, increasing the electrostatic stabilization by substituting the cationic charge of the potassium or sodium that would normally occupy this site.[44]

Among all the metal complexes, Ru(II) complexes have attracted considerable attention not only because of their DNA-binding properties, but also, more importantly, their "light switch" effects for DNA. In particular, $[Ru(bpy)_2dppz]^{2+}$ and $[Ru(phen)_2dppz]^{2+}$ (bpy = 2,2′-bipyridine, phen = 1,10-phenanthroline and dppz = dipyrido-[3,2-*a*:2′,3′-*c*] phenazine), known as the most famous DNA "light switch" complexes, have been studied a lot during the last decade.[45–47] Many experimental and theoretical methods have been carried out to elucidate the DNA "light switch" mechanism.[45,47–50] A detailed description of the "light switch" behavior remains elusive. One leading theory is that the "light switch" behavior results from the presence of two ^{3}MLCT states involving the dppz ligand: in aprotic solvents, the lowest ^{3}MLCT state is a bright state (BS) associated with the bipyridine (bpy) fragment and thus luminescence was observed, but in protic environments, the hydrogen bonding with the phenazine (phz) nitrogens lowered the energy of the dark state (DS), localized largely on the phz portion, to below that of the BS and quenched the luminescence by a decay process from the DS *via* nonradiative vibrational relaxation back to the ground state.[51]

Many Ru(II) complexes have been reported to intercalate between the duplex DNA base pairs and stabilize the ds-DNA.[52–54] Recently, our laboratory found that Ru(II) complexes can also serve as a prominent molecular "light switch" for G-quadruplexes.[55] Furthermore, we have described the first example of a new G-quadruplex DNA "light switch" complex, which can be repeatedly cycled on and off through the addition of external agents.[56] Nevertheless, most of the complexes have a low fluorescence enhancement with G-quadruplex DNA and can't be observed with the naked eye. Some of them exhibit residual emission in a DNA-free water solution or have a weak stabilization ability with the G-quadruplex structure.

In the present work, we report a new Ru(II) complex, $[Ru(bpy)_2dppz\text{-}idzo]^{2+}$ (dppz-idzo = dppz-10,11-imidazolone), as a molecular "light switch" for G-quadruplex DNA (22AG, $d[AGGG(TTAGGG)_3]$). The molecular structure is shown in Scheme 1. We introduced an imidazolone group to the main ligand (dppz) of the Ru-complex and dramatically enhanced the emission and selectivity to detect G-quadruplex DNA even with naked eye. Moreover, the stabilization of the G-quadruplex structure by $[Ru(bpy)_2dppz\text{-}idzo]^{2+}$ (complex **1**) was characterized in comparison with $[Ru(bpy)_2dppz]^{2+}$ (complex **2**). The G-quadruplex structure in a K^+ solution, which is considered to be biologically more relevant due to the higher intracellular concentration of K^+, is extensively investigated in this article. We hope that our research findings will be helpful for the understanding of G-quadruplex DNA recognition by Ru(II) complexes as well as laying the foundation for the rational design of new anticancer drug candidates.

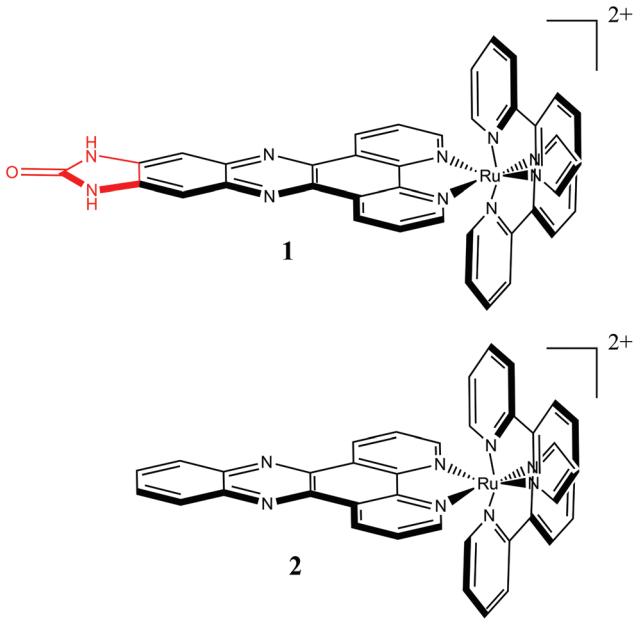

Scheme 1 Chemical structures of $[Ru(bpy)_2dppz\text{-}idzo]^{2+}$ (**1**) and $[Ru(bpy)_2dppz]^{2+}$ (**2**).

Experimental section

Materials

1,10-Phenanthroline-5,6-dione, 5,6-dinitrobenzimidazolone, 5,6-diaminobenzimidazolone and *cis*-$Ru(bpy)_2Cl_2{\cdot}2H_2O$ were synthesized according to the literature methods.[57–60] The other chemicals were obtained from commercial sources and used without further purification. The synthetic route to $[Ru(bpy)_2dppz\text{-}idzo]^{2+}$ is shown in Scheme 2 and the synthetic details are given below. The DNA oligomer 22AG (5′-AGGGTTAGGGTTAGGGTTAGGG-3′) and 22CT (5′-CCCT AACCCTAACCCTAACCCT-3) were purchased from Sangon (Shanghai, China). Calf thymus DNA (CT-DNA) was obtained from Sigma. The concentrations of these oligomer samples were determined by measuring the absorbance at 260 nm. Single-strand extinction coefficients were calculated from mononucleotide data using a nearest-neighbour approximation. The formation of an intramolecular G-quadruplex was performed according to the following procedures: the oligonucleotide samples dissolved in a K^+ buffer were heated to 90 °C for 5 minutes, gently cooled to room temperature and then incubated at 4 °C overnight. Buffer A: 10 mM tris-HCl, 100 mM KCl, pH 7.0; Buffer B: 10 mM KH_2PO_4–K_2HPO_4, 100 mM KCl, pH 7.0.

Synthesis of $[Ru(bpy)_2dppz\text{-}idzo]{\cdot}(PF_6)_2$

Benzimidazolone-2 (2). A mixture of 5.4 g (0.05 mol) of *o*-phenylenediamine, 3.4 g (0.057 mol) of urea and 25 mL of glycol were stirred for 1 h at 130–140 °C and then heated at a maximum temperature of 170 °C for 7 h. The solution was cooled down to 40–50 °C and 5 mL of 95% ethanol was added with stirring for 10 min and then 20 mL of distilled water was

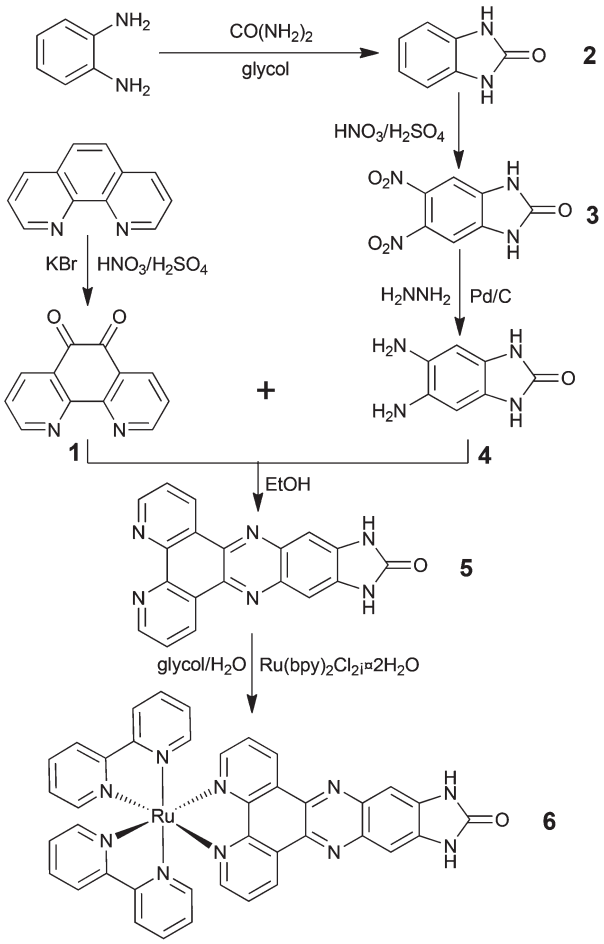

Scheme 2 Synthetic route to $[Ru(bpy)_2dppz\text{-}idzo]^{2+}$.

added. The precipitate was filtered and washed with successive batches of water and 95% ethanol. The residue was dried under vacuum to give 4.7 g of off-white benzimidazolone-2 in a yield of 70%.

5,6-Dinitrobenzimidazolone-2 (3). Benzimidazolone-2 (3.35 g, 25 mmol) was dissolved in 13 mL of 98% sulfuric acid. The colorless solution was cooled to 0–5 °C in an ice bath and 4 mL of 90% fuming nitric acid in 13 mL of 98% sulfuric acid was added dropwise to the cooled, stirred solution. The reaction temperature was not allowed to go above 5 °C during the addition. After that, the cold solution was rapidly poured onto 150 g of ice. The yellow precipitate was collected *via* filtration and washed thoroughly with cold water. After drying under vacuum, 4.2 g of yellow 5,6-dinitrobenzimidazolone-2 was obtained in a yield of 82%.

5,6-Diaminobenzimidazolone-2 (4). 10 mL of hydrazine hydrate (85%) was added dropwise to a mixture of 2.24 g (10 mmol) of **3** and 0.3 g of palladium on activated carbon (10% Pd/C) in 150 mL of refluxing water–methanol (1 : 2, v/v) within 5 min. The reaction mixture was refluxed for a further 4 h and then filtered while hot. After concentrating under vacuum, the off-white 5,6-diaminobenzimidazolone-2 was precipitated from the filtrate (1.2 g, yield 75%).

Dipyrido[3,2-*a*:2′,3′-*c*]phenazine-10,11-imidazolone-2 (dppz-idzo) (5). 0.27 g of 1,10-phenanthroline-5,6-dione (**1**) (1.28 mmol) was dissolved in 30 mL of ethanol with stirring. 0.21 g of 5,6-diaminobenzimidazolone-2 (1.28 mmol) was added to this solution and a yellow precipitate formed immediately. The reaction mixture was then refluxed for a further 15 min and the yellow solid was collected by filtration. After drying thoroughly, 0.4 g of dppz-idzo (**5**) was obtained in a yield of 90%.

[Ru(bpy)$_2$dppz-idzo]·(PF$_6$)$_2$ (6). 0.208 g of *cis*-[Ru(bpy)$_2$Cl$_2$]·2H$_2$O (0.4 mmol) and 0.21 g of dppz-idzo (0.60 mmol) were mixed in 40 ml of glycol–water (7 : 1, v/v). The mixture was refluxed for 6 h. Upon cooling, the reaction mixture was diluted with 40 mL of water and filtered to remove solid impurities. Then, 2 g of NH_4PF_6 was added to the filtrate and the crude product precipitate was dried and collected. The complex was then purified by alumina chromatography using MeCN–methanol (5 : 1, v/v) as the eluent and further recrystallized from acetone–diethyl ether (1 : 5, v/v). Yield: 240 mg, 56%. ^{1}H NMR [$(CD_3)_2SO$]: δ 11.71 (2H, s), 9.61 (2H, d), 8.88 (4H, dd), 8.22 (4H, m), 8.14 (2H, t), 8.01 (2H, dd), 7.84 (2H, d), 7.76 (4H, d), 7.60 (2H, t), 7.38 (2H, t). Calc. for $C_{39}H_{26}F_{12}N_{10}OP_2Ru$: C, 44.97; H, 2.52; N, 13.45. Found: C, 44.95; H, 2.53; N, 13.43. MALDI-MS: calcd For $C_{39}H_{26}N_{10}ORu$ 751.76 $[M]^+$; found 751.1 $[M]^+$.

General procedures

All synthetic reactions were performed under an argon atmosphere. Elemental analyses (C, H, and N) were performed on a Perkin-Elmer 240C elemental analyzer. The ^{1}H NMR spectra of Ru(bpy)$_2$dppz-idzo in $(CD_3)_2SO$ were collected on a Bruker ARX-400 NMR spectrometer. Matrix assisted laser desorption ionization mass spectra (MALDI-MS) were measured on an Ion Spec HiResMALDI spectrometer. The UV-visible absorption spectra were recorded on a Perkin-Elmer Lambda Bio 40 spectrometer. UV-visible, colorimetric and emission spectrophotometric measurements were carried out in buffer A. The CD measurements were performed in buffer B. Deionized water was used to prepare all the Ru(II) complex aqueous solutions.

Fluorescence titrations

Fluorescence spectra were measured on a Hitachi F-7000 fluorescence spectrophotometer at room temperature. The excitation wavelength was set at 460 nm and the emission spectrum was collected from 500 to 800 nm. The excitation and emission slits were both set at 10 nm. Luminescence titrations were performed as following: 2000 μL of 2.5 μM [Ru(bpy)$_2$(dppz-idzo)]$^{2+}$ in a 1.0 cm path length quartz cuvette was loaded into the fluorimeter sample block. After 5 min to allow the sample to equilibrate, the first spectrum was recorded and then 5 μL of a 100 μM DNA solution was added to the sample cell followed by thorough mixing. After 5 min, the spectrum was taken again. The titration processes were repeated until there was no apparent change in the spectra for at least four cycles, indicating the achievement of the binding saturation. The concentration of the bound compound was calculated using eqn (1)[61]

$$C_b = C_t[(F - F^0)/(F^{max} - F^0)] \quad (1)$$

where C_t is the total compound concentration, F is the observed fluorescence emission intensity at a given DNA concentration, F^0 is the intensity in the absence of DNA and F^{max} is the fluorescence of the totally bound compound. The affinity constant of the Ru-complex with G-quadruplex DNA was calculated using the Scatchard equation (eqn (2)).

$$r/C_f = -rK_a + nK_a \quad (2)$$

where r is the binding ratio $C_b/[DNA]_t$ and C_f is the free complex concentration, n is the number of binding sites per DNA molecule and K_a is the affinity constant. The luminescence quantum yields were calculated with reference to [Ru(bpy)$_3$]$^{2+}$ (φ_{std} = 0.028)[62,63] in aerated water at room temperature using eqn (3), where φ and φ_{std} are the quantum yields, A and A_{std} are the absorbance at the excitation wavelength and I and I_{std} are the integrated emission intensities for the unknown and standard samples, respectively.

$$\varphi = \varphi_{std}(A_{std}/A)(I/I_{std}) \quad (3)$$

Colorimetric experiments

In the colorimetric experiments, the final concentrations of the DNA and Ru-complexes were adjusted to 2.5 and 5.0 μM, respectively. The total volume of every sample was 2 mL. All the samples were photographed under irradiation with UV light (Vilber Lourmat, Bio-Print, VL) at 365 nm without any incubation.

Circular dichroism measurements

Circular dichroism (CD) titrations were performed on a Jasco J-810 spectropolarimeter at room temperature using a quartz cell with a 1 cm path length. The DNA (22AG) samples were dissolved in two different solutions in this study: (a) 10 mM tris-HCl, pH 7.0; (b) 100 mM KCl in a 10 mM PBS buffer, pH 7.0. The process of the CD titrations was similar to that of fluorescence titrations. The DNA samples, at a concentration of 2.5 μM, were dissolved in corresponding solutions and placed in a quartz cuvette (2000 μL of the sample). During the titrations, an aliquot (5 μL) of a [Ru(bpy)$_2$dppz-idzo]$^{2+}$ (200 μM) solution was added to the cuvette each time and mixed thoroughly. After a further equilibrium of 5 min, the CD spectra were recorded. The titration processes were repeated until there was almost no change in the spectra, indicating binding saturation had been achieved. For each sample, at least four spectrum scans were accumulated over the wavelength range of 225–350 nm at a scanning rate of 100 nm min^{-1}. During the measurement, the instrument was flushed continuously with dry nitrogen gas. The scan of the buffer alone (baseline) was subtracted from the average scan for each sample.

Thermal DNA denaturation experiments

The melting temperatures of the G-quadruplex DNA were measured by employing a Jasco J-810 spectropolarimeter equipped with a Peltier temperature-control programmer (±0.1) °C. DNA samples (2.5 μM) dissolved in buffer B were measured using a 1 cm path quartz cell in the absence and presence of 5 μM Ru-complexes, respectively. Melting plots were collected by a CD signal as a function of temperature. Characteristic signals of the quadruplex DNA were measured at 295 nm.[64] The temperature was increased from 40 to 90 °C at the rate of 1 °C min^{-1}.

Theoretical calculations

$[Ru(bpy)_2dppz\text{-}idzo]^{2+}$ is made of one Ru(II) atom, one main ligand (dppz-idzo) and two ancillary ligands (bpy), as shown in Scheme 1. There are 77 atoms involved in the complex, which has C_1 symmetry. The geometric and energy optimizations for the ground states of $[Ru(bpy)_2dppz\text{-}idzo]^{2+}$ were performed with the Gaussian 03 program based on the density functional theory (DFT) method.[65] The subsequent frequency analysis shows that the structure is a local minima on the potential energy surface. Vertical singlet transition energies of the Ru(II) complex were also obtained using time-dependent DFT (TDDFT).[66–68] All the calculations were performed by employing Becke's three parameter hybrid functional with the Lee–Yang–Parr correlation functional (B3LYP) method.[69–71] The DFT calculations with the B3LYP method have been shown to be very effective for bio-molecular interactions, such as DNA–small molecule interactions.[72] Thus, we have adopted this method for our investigations. The LANL2DZ basis set was used to treat the Ru atom, whereas the 6-31G* basis set was used to treat all the other atoms (C, N, O, H).[73,74] To clarify the nature of the excited state, orbital analysis of the complexes were also performed.

Molecular docking

The electronic structure of $[Ru(bpy)_2dppz\text{-}idzo]^{2+}$ was optimized using the DFT-B3LYP method with the 6-31G* basis set for the C, N, O, H atoms and LanL2DZ for the Ru atom with the G03 quantum chemistry program-package. The hybrid-type mixed parallel/antiparallel G-quadruplex structure in a K^+ solution was obtained from the protein data bank (PDB ID: 2HY9) as an initial model to study the interaction between $[Ru(bpy)_2(dppz\text{-}idzo)]^{2+}$ and the 22AG telomeric DNA. Before docking, necessary modifications were carried out according to a literature report.[56] Two adenines located at the end of the initial model were removed and slight modifications to increase the separation between loop base pairs and the G-quartet were performed, as reported in the literature.[75] The molecular docking was performed with the AutoDock 4.2 Lamarckian Genetic Algorithm (LGA).[76–78] In the automated molecular docking process, a DNA molecule was enclosed in a 60 Å cubic grid created by the AutoGrid algorithm (a subprogram of AutoDock) with 0.375 Å spacing and the default parameters (supplied with the program package) were used for dispersion/repulsion, hydrogen bonding, electrostatics and desolvation. The LGA in AutoDock 4.2 was applied to search for the conformational and orientational space of the Ru(II)-complex while keeping the G-quadruplex structure rigid. AutoGrid performed precalculated atomic affinity grid maps for each atom type in the ligand plus an electrostatics map and a separate desolvation map present in the substrate molecule. Then, during the AutoDock calculation, the energetics of a particular ligand configuration was evaluated using the values from the grids. Finally, the Ru(II)–DNA docked complex was selected according to the criteria of interacting energies matched with geometric quality. The output from AutoDock was imported into Accelrys Discovery Studio 2.5 Client for further rendering.[79]

Results and discussion

Synthesis of the complex

The synthetic procedure for the complex $[Ru(bpy)_2dppz\text{-}idzo]^{2+}$ includes mainly four steps: (1) the 5,6-dinitrobenzimidazolone-2 was synthesized through cyclization and nitration reactions, as reported by Zehui Yang,[58] (2) the 5,6-diaminobenzimidazolone-2 was synthesized through catalysis hydrogenation by Pd/C,[59] (3) a moderate condensation reaction of 5,6-diaminobenzimidazolone-2 with 1,10-phenanthroline-5,6-dione rapidly produced the main ligand dppz-idzo,[67] (4) the final product was synthesized through the coordination between the main ligand dppz-idzo and the precursor complex $[Ru(bpy)_2Cl_2]\cdot 2H_2O$. After further purification, the complex was obtained with good purity and a relatively high yield. The structure was characterized by ^1H NMR, MALDI-MS and elemental analysis.

Fluorescent and colorimetric studies

The fluorescence behaviour of $[Ru(bpy)_2dppz\text{-}idzo]^{2+}$ (**1**) and $[Ru(bpy)_2dppz]^{2+}$ (**2**) with the G-quadruplex DNA structure were investigated. The effects of successive additions of 22AG DNA on the emission spectra of the Ru-complexes are depicted in Fig. 2. It was clear that in the absence of the DNA, both the complexes were almost nonemissive. Upon successive additions of the DNA, the luminescence of complex **1** and **2** rose sharply by about 300- and 80-fold enhancements in the emission intensity ($I/I_0 \approx 300$ and 80, $\varphi = 0.067$ and 0.020) at [DNA]/[Ru] = 1.0 ([DNA] = [Ru] = 2.5 μM), respectively, behaving like DNA molecular "light switches". These emission changes of the Ru(II) complexes induced by the addition of the DNA clearly indicate that they are bound to the G-quadruplex structure. Based on the emission enhancement, the intrinsic binding constant (K_b) of each complex was obtained according to the Scatchard equation. The values of the binding constant were about 4.8×10^6 and 2.3×10^6 for complex **1** and **2**, respectively.

The binding stoichiometry was determined by utilizing the method of continuous variation analysis (Job plot). The total concentrations of DNA and Ru-complexes were held constant,

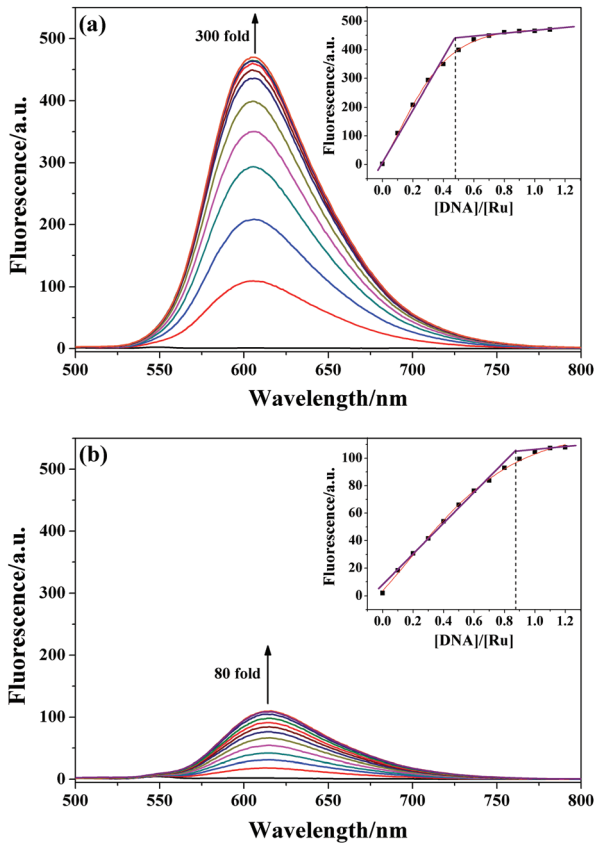

Fig. 2 Changes in the emission spectra (λ_{ex} = 460 nm) of 2.5 μM $[Ru(bpy)_2dppz\text{-}idzo]^{2+}$ (a) and $[Ru(bpy)_2dppz]^{2+}$ (b) with increasing concentrations of 22AG DNA (0–3.0 μM) in 10 mM tris-HCl, 100 mM KCl, pH 7.0. Insets: plots of *I vs.* [DNA]/[Ru] and the best fit for the titrations of Ru(II) complexes with 22AG DNA.

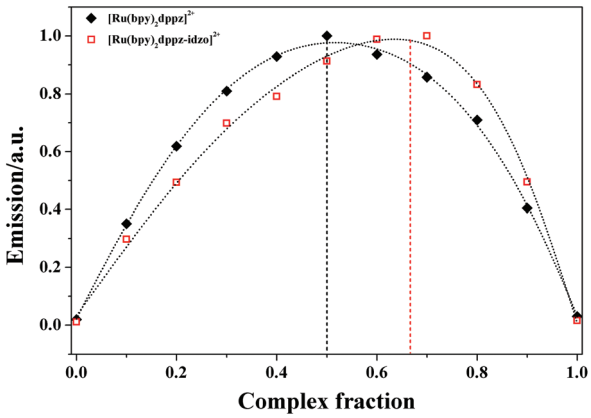

Fig. 3 Job plots constructed from mixing the Ru-complexes and 22AG together in variable ratios but a constant total concentration (2.5 μM) in a K^+ buffer (10 mM tris-HCl, 100 mM KCl, pH 7.0). The normalized peak values of the emission are plotted *versus* the fraction of the Ru-complex ($[Ru(bpy)_2dppz\text{-}idzo]^{2+}$ (□) and $[Ru(bpy)_2dppz]^{2+}$ (◆)).

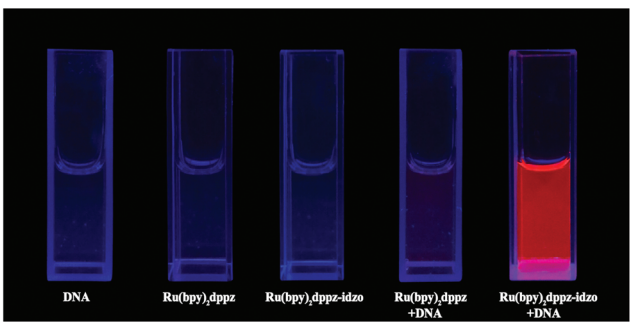

Fig. 4 Images of the "light switch" behavior of Ru(II) complexes (5 μM) for DNA (2.5 μM) under UV light at 365 nm in 10 mM tris-HCl, 100 mM KCl, pH 7.0.

while the relative molar ratios changed for each sample, from 0 : 1 (all DNA) to 1 : 0 (all complex). The emission data at 605 nm and 615 nm were used to generate Job plots for complex **1** and **2**, respectively. As shown in Fig. 3, it is clear that two molecules of complex **1** bind to each molecule of the G-quadruplex, whereas only one molecule of complex **2** binds to a molecule of the G-quadruplex.

UV-visible titrations were also carried out to investigate the interaction between the complexes and 22AG in a K^+ solution (see Fig. S1 and S2, ESI†). Both complexes exhibited apparent hypochromism in the absorption band. Based on the absorption results, the binding constants of **1** and **2** towards hybrid-type G-quadruplex DNA were calculated to be 3.17×10^6 and 1.69×10^6, respectively. These values were comparable to those obtained from fluorescence titrations.

The strong enhancement of the intrinsic fluorescence of $[Ru(bpy)_2dppz\text{-}idzo]^{2+}$ when bound to DNA provides a possibility for the visual detection of the G-quadruplex structure. As shown in Fig. 4, this dramatic "light switch" effect can easily be observed by the naked eye under UV light. The results show that $[Ru(bpy)_2dppz\text{-}idzo]^{2+}$ is a prominent colorimetric molecular "light switch" for 22AG DNA in a K^+ solution. The limit of detection (LOD) for the G-quadruplex with this "switch on" assay can reach upto 6 nM at a signal-to-noise ratio of 3 (S/N = 3). In addition, the selectivity of the title complex towards the G-quadruplex DNA structure was also studied using fluorescence measurements and the results are shown in Fig. 5. We can see that our complex displayed specificity towards the G-quadruplex in a K^+ solution, indicating a potential application in the visual detection of a hybrid-type G-quadruplex structure. The fluorescence titration of the title complex with ds-DNA (calf thymus DNA, CT-DNA) was also investigated (Fig. S3, ESI†) and the luminescence selectivity results are shown in Fig. S4 in the ESI.† It is obvious that the title complex showed a good fluorescence selectivity towards quadruplex over duplex DNA when both of them were at the same concentration ([G4] = [CT] = [Ru] = 2.5 μM), while a modest selectivity for quadruplex over duplex was observed when the amount of ds-DNA was much larger than that of the quadruplex DNA ([CT] = 12.5 μM > [G4] = 2.5 μM). Furthermore, a competition dialysis assay was also conducted to investigate the quadruplex selectivity in the binding affinity according to the literature.[80,81] As shown in Fig. S5, ESI† $[Ru(bpy)_2dppz\text{-}idzo]^{2+}$ showed good binding selectivity towards quadruplex over duplex DNA at the same DNA concentration,

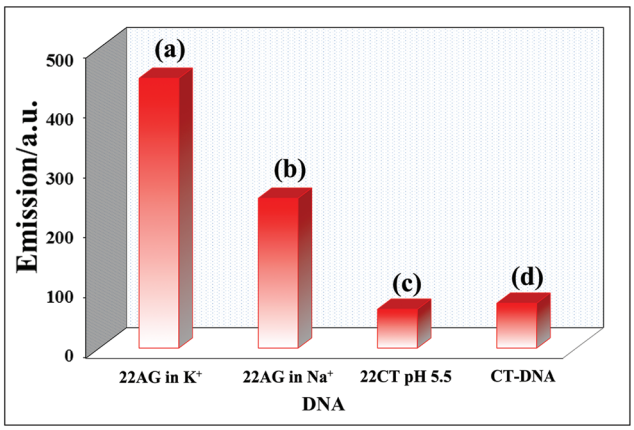

Fig. 5 Specific luminescent selectivity of $[Ru(bpy)_2dppz\text{-}idzo]^{2+}$ towards hybrid G-quadruplex. The concentration of the Ru complex and DNAs was 2.5 μM. Buffer of each sample: (a) 10 mM tris-HCl, 100 mM KCl, pH 7.0; (b) 10 mM tris-HCl, 100 mM NaCl, pH 7.0; (c) 10 mM tris-HCl, 100 mM NaCl, pH 5.5; (d) 10 mM tris-HCl, 50 mM NaCl, 1 mM EDTA, pH 7.5.

while still displaying moderate selectivity towards G-quadruplex DNA even in the presence of a vast amount of ds-DNA.

Computational studies

To further investigate the mechanism of the light-switch effect, DFT and time-dependent DFT (TD-DFT) calculations were performed for $[Ru(bpy)_2dppz\text{-}idzo]^{2+}$. The selected calculated coordination dihedral angles are shown in the ESI (Table S1†). We can see that the imidazolone group is coplanar with dppz in $[Ru(bpy)_2dppz\text{-}idzo]^{2+}$, with the dihedral angles close to 180.00°. The distributions of the frontier molecular orbitals obtained by the DFT calculations are shown in Fig. 6. The highest occupied molecular orbital (HOMO), the HOMO − 1 and HOMO − 2 are primarily characterized by the d orbitals of the Ru atom with a small distribution on the ligands. The HOMO − 3 resides on both the ruthenium center and the main ligand (dppz-idzo). Its lowest unoccupied molecular orbital (LUMO) is distributed over the whole dppz-idzo ligand ($\pi^*_{dppz\text{-}idzo}$). The LUMO + 1 and LUMO + 2 are mainly located on the ancillary ligands (π^*_{bpy}), while the LUMO + 3 receives a dominant contribution from the proximal bpy portion of dppz-idzo.

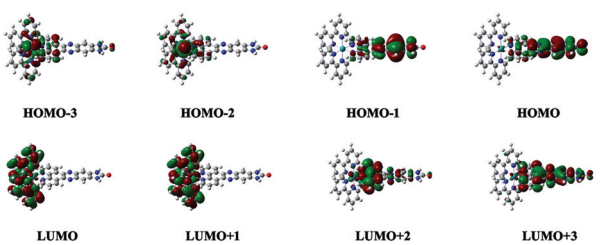

Fig. 6 Contour plots of some selected frontier molecular orbitals of $[Ru(bpy)_2dppz\text{-}idzo]^{2+}$.

The electronic absorption spectra of $[Ru(bpy)_2dppz\text{-}idzo]^{2+}$ in neutral water in the vertical singlet excited states were also calculated by TD-DFT at the B3LYP//LanL2DZ/6-31G* level. The transition results of the six calculated lowest-lying excited singlet states are shown in Table 1. The transition contributions show that all of the five excited states in this table are ^{1}MLCT in character. The lowest-energy ^{1}MLCT state of the complex was calculated to be at 2.70 eV (459.33 nm). Based on the calculated oscillator strength, the measured low-energy absorption band of $[Ru(bpy)_2dppz\text{-}idzo]^{2+}$ at 450 nm is assigned to the ES1 (459 nm), ES2 (452 nm) and ES3 (452 nm) states, which are mainly composed of the HOMO → LUMO/LOMO + 1/LOMO + 3 transitions. The calculated absorption band is very close to the experimental data (Fig. 7). According to the orbital distributions, these transitions originate mainly from d_{Ru} orbits to $\pi^*_{dppz\text{-}idzo}$, with a small contribution from d_{Ru} orbits to π^*_{bpy}. In addition, the ES4 (430 nm), ES5 (428 nm) and ES6 (424 nm) states, characterized by relatively higher energy and oscillator strength, are responsible for the experimentally observed stronger absorption band at 400 nm. These ^{1}MLCT states are mainly assigned to the HOMO − 1/HOMO − 2 → LUMO/LUMO + 1/LUMO + 3 transitions.

It has been reported that charge transfer from a central Ru(II) atom to the distal phz part of the dppz ligand gives rise to a nonemissive state, whereas the emissive state arises from the MLCT transition from Ru(II) to the proximal bpy of the dppz ligand or the ancillary ligands.[45,48,49,51,82] In a water solution, hydrogen bonding between the phz nitrogen and the solvent would lead to the decay of the excited state *via* nonradiative vibrational relaxation back to the ground state and quench the luminescence. Therefore, the key factor that determines the BS/DS property of an excited state is whether the excited state has the phz nitrogen atomic orbital's character or not. For $[Ru(bpy)_2dppz\text{-}idzo]^{2+}$, the electron density of the LUMO + 2 is localized on the proximal bpy portion of the dppz-idzo and all the other LUMOs (LUMO, LUMO + 1 and LUMO + 3) contain phz nitrogen atomic orbitals. Thus, the transitions from Ru(II) to LUMO + 2 would result in an emissive MLCT excited state, whereas the MLCT excited states involving the LUMO, LUMO + 1 and LUMO + 3 should be nonemissive or weakly emissive. In addition, it has been proposed that the MLCT states possessing >75% of the nonemissive transitions should be assigned to DSs, as BSs contained only emissive transitions, and all the others should be labelled mixed-states (MS).[82] On the basis of the transition contributions and the coefficients of the singlet excited states shown in Table 1, we can conclude that all the listed excited states belong to DSs. This should be responsible for the nonemissive state of the Ru(II) complex in water without DNA. DFT/TD-DFT calculations of the free Ru-complex molecule without water as a solvent were also performed and the results are shown in the ESI (Fig. S6, Table S2†). We can see that the first three excited states (ES1, ES2 and ES3) are BSs, while ES4 and ES5 are MSs and only ES6 is DS. This is the explanation for the fluorescence enhancement of $[Ru(bpy)_2dppz\text{-}idzo]^{2+}$ under the protection of G-quadruplex DNA.

Table 1 TD-DFT calculated energies, oscillator strengths, transition contributions, and coefficients of the six lowest-energy excited singlet states of $[Ru(bpy)_2dppz\text{-}idzo]^{2+}$ at the B3LYP//Lanl2dz/6-31G* level

Excited state	λ_{abs}/nm (eV)	Oscillator strength	Transition contribution	Coefficient
ES1	459.33(2.70)	0.0000	HOMO → LUMO	0.5111(52.24%)
			HOMO → LUMO + 1	0.1834(6.73%)
			HOMO → LUMO + 3	−0.4486(40.25%)
ES2	452.26(2.74)	0.0000	HOMO → LUMO + 3	0.6974(97.28%)
ES3	452.24(2.74)	0.0007	HOMO → LUMO + 1	0.6231(77.65%)
			HOMO → LUMO + 3	0.3171(20.11%)
ES4	430.51(2.88)	0.2430	HOMO − 3 → LUMO + 1	0.1136(2.58%)
			HOMO − 1 → LUMO	0.5950(70.81%)
			HOMO − 1 → LUMO + 1	0.3201(20.49%)
			HOMO − 1 → LUMO + 3	−0.1239(3.07%)
ES5	428.28(2.89)	0.0026	HOMO − 2 → LUMO	0.4737(44.87%)
			HOMO − 2 → LUMO + 1	0.1119(2.50%)
			HOMO − 2 → LUMO + 3	−0.4349(37.83%)
			HOMO − 1 → LUMO + 2	−0.2185(9.55%)
ES6	424.00(2.92)	0.0020	HOMO − 3 → LUMO + 2	0.1618(5.23%)
			HOMO − 2 → LUMO	0.1220(2.98%)
			HOMO − 2 → LUMO + 3	0.2887(16.67%)
			HOMO − 1 → LUMO + 1	0.4269(36.45%)
			HOMO → LUMO + 2	0.2905(16.88%)
			HOMO → LUMO	−0.1843(6.79%)
			HOMO → LUMO + 3	0.2455(12.05%)

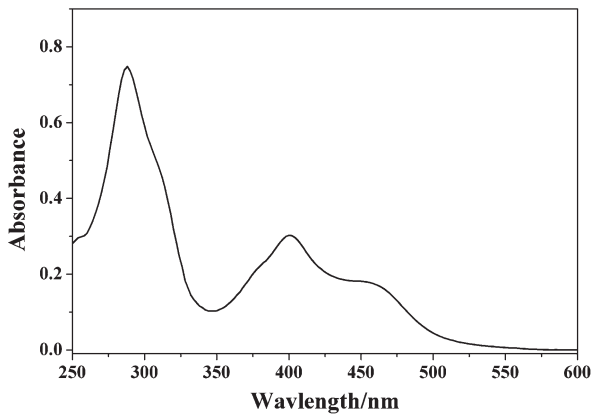

Fig. 7 Experimental electronic absorption spectra of $[Ru(bpy)_2dppz\text{-}idzo]^{2+}$ (10 μM) at room temperature in pure water.

CD measurements

Circular dichroism (CD) spectroscopy, which is extremely useful in conformational studies, is widely used to study the conformations of G-quadruplexes.[83] It has been reported that the CD spectra of 22AG without any metal cations exhibits a major positive band at 257 nm, a negative band centered at 235 nm and a minor negative band at 280 nm, which probably corresponds to the random coil structure.[84,85] Upon the titration of 22AG with increasing amounts of the title complex in a free cation aqueous solution, a dramatic change in the CD spectrum was observed (Fig. 8a). With the successive addition of $[Ru(bpy)_2dppz\text{-}idzo]^{2+}$, the major positive band at 257 nm gradually decreased and shifted to 245 nm, the negative band at 235 nm disappeared, the minor negative band at 280 nm slightly increased and moved to 265 nm and the small positive band at 295 nm clearly increased. These changes in the CD signals indicate a significant conformational conversion.

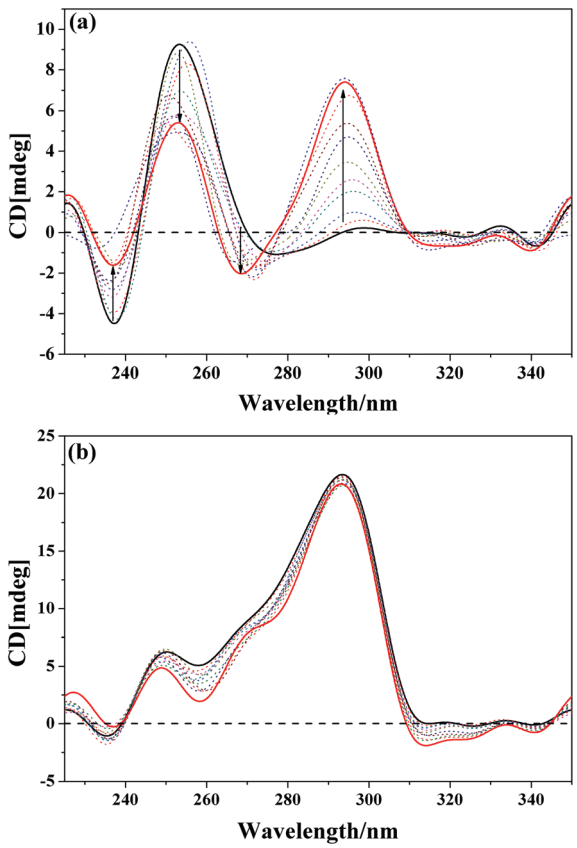

Fig. 8 CD titrations of 22AG (2.5 μM) by adding $[Ru(bpy)_2dppz\text{-}idzo]^{2+}$ (a) in a tris buffer without metal ions (10 mM tris-HCl, pH 7.0) and (b) in a K^+ buffer (10 mM KH_2PO_4–K_2HPO_4, 100 mM KCl, pH 7.0) at room temperature. The concentrations of the Ru-complex range from 0 (solid black) to 5 μM (solid red).

As the concentration of the title complex increased to 5 μM, the CD spectrum of this new DNA conformation was almost

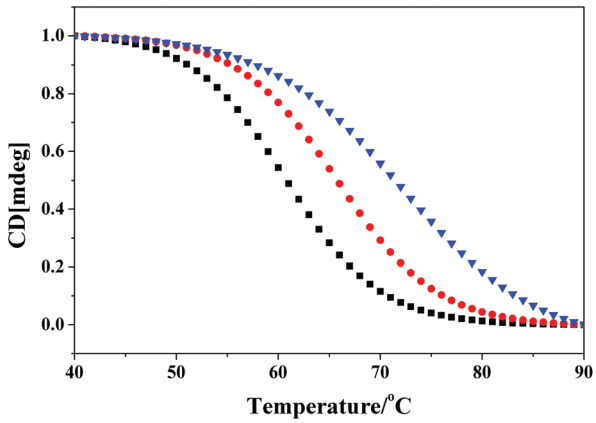

Fig. 9 Normalized melting curves of the G-quadruplex DNA (2.5 μM) measured by circular dichroism in a K^+ buffer (10 mM KH_2PO_4–K_2HPO_4, 100 mM KCl, pH 7.0) in the absence of the Ru(II) complex (■), in the presence of 5 μM $[Ru(bpy)_2dppz]^{2+}$ (●) and 5 μM $[Ru(bpy)_2dppz\text{-}idzo]^{2+}$ (▼), respectively.

identical to that of the antiparallel G-quadruplex structure described in previous researches, which was characterized by a major positive peak at 295 nm with a smaller negative peak at 265 nm and a positive peak at 245 nm.[8,86] This indicates that the title complex is capable of promoting the formation of the human telomeric intramolecular G-quadruplex structure independently without any other metal ions.

The structures and stability of the G-quadruplex DNA are largely influenced by the presence of monocations, especially Na^+ and K^+. Due to the higher intracellular concentration of K^+, the G-quadruplex in a K^+ solution was considered to be biologically more relevant and introduced to investigate the interaction with the title Ru(II) complex. As shown in Fig. 8b, in the absence of the Ru(II) complex, 22AG adopted a typical hybrid-type G-quadruplex structure in a K^+ buffer, exhibiting a distinct CD spectrum containing a strong positive peak at 295 nm with a shoulder peak around 268 nm and a smaller negative peak at 235 nm.[8,84] After successive additions of $[Ru(bpy)_2dppz\text{-}idzo]^{2+}$, no apparent changes were observed in the CD spectrum, indicating that the interaction between the title complex and the DNA hardly changed the G-quadruplex structure in a K^+ solution.

Thermal melting experiments were also performed, employing the circular dichroism to demonstrate the stabilization of hybrid G-quadruplex DNA by the Ru(II) complexes. The normalized thermal denaturation profiles of 22AG in a K^+ buffer are depicted in Fig. 9. It should be noted that $T_{1/2}$ is used instead of T_m to describe the transition temperature as G-quadruplex DNA–ligand interactions are not reversible.[64] As shown in Fig. 9, the $T_{1/2}$ of 2.5 μM 22AG in a K^+ solution increased from 60.7 to 72.2 °C in the presence of 5 μM $[Ru(bpy)_2dppz\text{-}idzo]^{2+}$ and increased to 65.8 °C in the presence of $[Ru(bpy)_2dppz]^{2+}$. The enhancements in $T_{1/2}$ of the G-quadruplex DNA indicated that both Ru complexes stabilized the G-quadruplex structure in a K^+ buffer. Obviously the title complex exhibited a much more powerful stabilization ability than the classic $[Ru(bpy)_2dppz]^{2+}$ complex according to the significant increase in the melting temperature of the G-quadruplex.

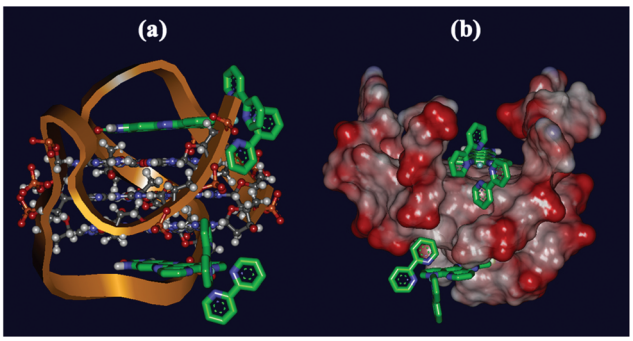

Fig. 10 The calculated model of $[Ru(bpy)_2dppz\text{-}idzo]^{2+}$ binding to the mixed hybrid-type G-quadruplex DNA. (a) The G-quartets are displayed in a ball and stick mode; (b) the G-quadruplex is rendered with a solvent surface and colored by interpolated charge.

Molecular docking

Finally, molecular docking simulations were carried out to get an insight into the interaction between $[Ru(bpy)_2dppz\text{-}idzo]^{2+}$ and the G-quadruplex. The structure of the title complex was optimized on the basis of the DFT-B3LYP method using Gaussian03. The mixed hybrid-type G-quadruplex was obtained from the protein data bank (PDB entry: 2HY9) as a template for the docking studies. Two extra adenines were removed from each end of the 26-mer mixed hybrid-type structure before docking, according to the literature.[75] The results of the Job plot (Fig. 3) indicate that every G-quadruplex molecule probably binds with two molecules of the title complex. As shown in Fig. 10, the docking study confirms that each intramolecular G-quadruplex molecule binds to two molecules of $[Ru(bpy)_2(dppz\text{-}idzo)]^{2+}$. It has been suggested that "End pasting" was a possible model of the interaction between many metal complexes and G-quadruplexes. This means the binders commonly stack on the surface of either the 5′- or 3′-terminal G-quartet plane.[31,38,56,87] Our results reveal that $[Ru(bpy)_2(dppz\text{-}idzo)]^{2+}$ probably bound to the mixed hybrid-type G-quadruplex structure at both termini (5′ and 3′ terminus) with potential π–π stacking interactions. This strong interaction and quite different binding model might result from the introduction of an imidazolone group to the main ligand of the Ru-complex, which effectively extended the square π-aromatic surface. This "sandwich-like" end-stacking of the title Ru(II) complex onto the G-quartets surfaces explained why its quadruplex stabilization ability was much stronger than that of the classic $[Ru(bpy)_2dppz]^{2+}$ complex.

Conclusions

Our previous investigations of the interactions between Ru(II) complexes and G-rich DNA showed that many of the complexes can serve as a prominent "light switch" for G-quadruplex structures, especially for the mixed hybrid-type quadruplex.[55,56,85]

However, most of the complexes exhibit a relatively low quantum yield with G-quadruplex DNA and can hardly be observed with the naked eye. Herein, a novel Ru(II) complex, $[Ru(bpy)_2dppz\text{-}idzo]^{2+}$, has been synthesized and characterized. The fluorescence titrations showed that the title compound acted as an excellent molecular "light switch" for hybrid-type G-quadruplex DNA (φ = 0.067), which was superior to the well-known DNA molecular "light switch" $[Ru(bpy)_2dppz]^{2+}$ (φ = 0.020). The title complex bonds to G-quadruplex DNA with a binding constant of 4.8×10^6 M^{-1} in a 10 mM tris-HCl, 100 mM KCl (pH = 7.0) buffer solution, as evidenced by UV-visible absorption and luminescence titrations. The geometry optimizations and computations of the electronic structure by applying the DFT-B3LYP method at the LanL2DZ/6-31G* level revealed that the idzo (imidazolone) group is coplanar with the dppz ring, which is in favour of the π stacking interactions between DNA quadruplexes and the Ru-complex.[88,89] The DFT/TD-DFT calculated ground- and vertical singlet excited-states for $[Ru(bpy)_2dppz\text{-}idzo]^{2+}$ provided a reasonable explanation for the "light switch" mechanism.

CD titrations have revealed that $[Ru(bpy)_2dppz\text{-}idzo]^{2+}$ can induce a significant conformational transition from a random coil to an antiparallel G-quadruplex structure independently in the absence of monocations (K^+ or Na^+). Moreover, the remarkable increase of the DNA melting temperature indicated that the title complex is a prominent stabilizer for the mixed hybrid G-quadruplex structure.

Based on the experimental results, an interesting "sandwich-like" binding model, characterized by one title molecule "pasting" onto each terminus of the G-quadruplex, was established through molecular docking simulations. This special interaction model may be responsible for the powerful stabilization ability of $[Ru(bpy)_2dppz\text{-}idzo]^{2+}$, superior to the well-known "light switch" $[Ru(bpy)_2dppz]^{2+}$.

The present results should be of value in systematical investigations of the interaction between G-quadruplexes and metal complexes as well as offer worthful experimental information for designing colorimetric probes and new anticancer therapeutics. Studies are in progress to determine the detailed biological activities of this complex.

Acknowledgements

This work was supported by the National Natural Science Foundation of China (20901060, 31170776 and 81171646) and the Fundamental Research Funds for the Central Universities.

Notes and references

1 J. Mohanty, N. Barooah, V. Dhamodharan, S. Harikrishna, P. I. Pradeepkumar and A. C. Bhasikuttan, *J. Am. Chem. Soc.*, 2012, **135**, 367–376.
2 J. T. Davis, *Angew. Chem., Int. Ed.*, 2004, **43**, 668–698.
3 S. Neidle and G. Parkinson, *Nat. Rev. Drug Discovery*, 2002, **1**, 383–393.
4 D. Sen and W. Gilbert, *Nature*, 1988, **334**, 364–366.
5 W. I. Sundquist and A. Klug, *Nature*, 1989, **342**, 825–829.
6 K. Guo, A. Pourpak, K. Beetz-Rogers, V. Gokhale, D. Sun and L. H. Hurley, *J. Am. Chem. Soc.*, 2007, **129**, 10220–10228.
7 Y. Wang and D. J. Patel, *Structure*, 1993, **1**, 263–282.
8 A. Ambrus, D. Chen, J. Dai, T. Bialis, R. A. Jones and D. Yang, *Nucleic Acids Res.*, 2006, **34**, 2723–2735.
9 K. N. Luu, A. T. Phan, V. Kuryavyi, L. Lacroix and D. J. Patel, *J. Am. Chem. Soc.*, 2006, **128**, 9963–9970.
10 T. Mashimo, H. Yagi, Y. Sannohe, A. Rajendran and H. Sugiyama, *J. Am. Chem. Soc.*, 2010, **132**, 14910–14918.
11 S. Balasubramanian, L. H. Hurley and S. Neidle, *Nat. Rev. Drug Discovery*, 2011, **10**, 261–275.
12 D. Sen and W. Gilbert, *Nature*, 1988, **334**, 364–366.
13 E. H. Blackburn, *Cell*, 2001, **106**, 661–673.
14 M. A. Blasco, *Carcinogenesis*, 2004, **25**, 1083–1087.
15 V. L. Makarov, Y. Hirose and J. P. Langmore, *Cell*, 1997, **88**, 657–666.
16 W. E. Wright, V. M. Tesmer, K. E. Huffman, S. D. Levene and J. W. Shay, *Genes Dev.*, 1997, **11**, 2801–2809.
17 A. T. Phan and J. L. Mergny, *Nucleic Acids Res.*, 2002, **30**, 4618–4625.
18 A. M. Zahler, J. R. Williamson, T. R. Cech and D. M. Prescott, *Nature*, 1991, **350**, 718–720.
19 P. Phatak, J. C. Cookson, F. Dai, V. Smith, R. B. Gartenhaus, M. F. G. Stevens and A. M. Burger, *Br. J. Cancer*, 2007, **96**, 1223–1233.
20 M. A. Blasco, *Eur. J. Cell Biol.*, 2003, **82**, 441–446.
21 A. M. Burger, *BioDrugs*, 1999, **12**, 413–422.
22 L. R. Kelland, *Eur. J. Cancer*, 2005, **41**, 971–979.
23 A. M. Burger, *Cancer Lett.*, 2007, **245**, 11–21.
24 P. J. Perry, M. A. Read, R. T. Davies, S. M. Gowan, A. P. Reszka, A. A. Wood, L. R. Kelland and S. Neidle, *J. Med. Chem.*, 1999, **42**, 2679–2684.
25 J.-L. Mergny, L. Lacroix, M.-P. Teulade-Fichou, C. Hounsou, L. Guittat, M. Hoarau, P. B. Arimondo, J.-P. Vigneron, J.-M. Lehn, J.-F. Riou, T. Garestier and C. Hélène, *Proc. Natl. Acad. Sci. U. S. A.*, 2001, **98**, 3062–3067.
26 F. Koeppel, J.-F. Riou, A. Laoui, P. Mailliet, P. B. Arimondo, D. Labit, O. Petitgenet, C. Hélène and J.-L. Mergny, *Nucleic Acids Res.*, 2001, **29**, 1087–1096.
27 A. K. Todd, M. Johnston and S. Neidle, *Nucleic Acids Res.*, 2005, **33**, 2901–2907.
28 J. L. Huppert and S. Balasubramanian, *Nucleic Acids Res.*, 2005, **33**, 2908–2916.
29 P. S. Shirude, L. Ying and S. Balasubramanian, *Chem. Commun.*, 2008, 2007–2009.
30 J. L. Huppert and S. Balasubramanian, *Nucleic Acids Res.*, 2007, **35**, 406–413.
31 P. Wang, C.-H. Leung, D.-L. Ma, S.-C. Yan and C.-M. Che, *Chem.–Eur. J.*, 2010, **16**, 6900–6911.
32 K. I. E. McLuckie, Z. A. E. Waller, D. A. Sanders, D. Alves, R. Rodriguez, J. Dash, G. J. McKenzie, A. R. Venkitaraman

and S. Balasubramanian, *J. Am. Chem. Soc.*, 2011, **133**, 2658–2663.
33 S. L. Palumbo, S. W. Ebbinghaus and L. H. Hurley, *J. Am. Chem. Soc.*, 2009, **131**, 10878–10891.
34 S. Kumari, A. Bugaut, J. L. Huppert and S. Balasubramanian, *Nat. Chem. Biol.*, 2007, **3**, 218–221.
35 Y. Xu, K. Kaminaga and M. Komiyama, *J. Am. Chem. Soc.*, 2008, **130**, 11179–11184.
36 A. Bugaut and S. Balasubramanian, *Nucleic Acids Res.*, 2012, **40**, 4727–4741.
37 G. W. Collie and G. N. Parkinson, *Chem. Soc. Rev.*, 2011, **40**, 5867–5892.
38 D.-L. Ma, C.-M. Che and S.-C. Yan, *J. Am. Chem. Soc.*, 2008, **131**, 1835–1846.
39 C. Yu, K. H.-Y. Chan, K. M.-C. Wong and V. W.-W. Yam, *Chem. Commun.*, 2009, 3756–3758.
40 S. Shi, J. Liu, T. Yao, X. Geng, L. Jiang, Q. Yang, L. Cheng and L. Ji, *Inorg. Chem.*, 2008, **47**, 2910–2912.
41 J. Talib, C. Green, K. J. Davis, T. Urathamakul, J. L. Beck, J. R. Aldrich-Wright and S. F. Ralph, *Dalton Trans.*, 2008, 1018–1026.
42 H. Bertrand, D. Monchaud, A. De Cian, R. Guillot, J.-L. Mergny and M.-P. Teulade-Fichou, *Org. Biomol. Chem.*, 2007, **5**, 2555–2559.
43 J. E. Reed, A. A. Arnal, S. Neidle and R. Vilar, *J. Am. Chem. Soc.*, 2006, **128**, 5992–5993.
44 S. N. Georgiades, N. H. Abd Karim, K. Suntharalingam and R. Vilar, *Angew. Chem., Int. Ed.*, 2010, **49**, 4020–4034.
45 M. K. Brennaman, T. J. Meyer and J. M. Papanikolas, *J. Phys. Chem. A*, 2004, **108**, 9938–9944.
46 S. Fantacci, F. De Angelis, A. Sgamellotti, A. Marrone and N. Re, *J. Am. Chem. Soc.*, 2005, **127**, 14144–14145.
47 E. R. Batista and R. L. Martin, *J. Phys. Chem. A*, 2005, **109**, 3128–3133.
48 E. J. C. Olson, D. Hu, A. Hörmann, A. M. Jonkman, M. R. Arkin, E. D. A. Stemp, J. K. Barton and P. F. Barbara, *J. Am. Chem. Soc.*, 1997, **119**, 11458–11467.
49 M. K. Brennaman, J. H. Alstrum-Acevedo, C. N. Fleming, P. Jang, T. J. Meyer and J. M. Papanikolas, *J. Am. Chem. Soc.*, 2002, **124**, 15094–15098.
50 J. Olofsson, B. Önfelt and P. Lincoln, *J. Phys. Chem. A*, 2004, **108**, 4391–4398.
51 A.-G. Zhang, Y.-Z. Zhang, Z.-M. Duan, K.-Z. Wang, H.-B. Wei, Z.-Q. Bian and C.-H. Huang, *Inorg. Chem.*, 2011, **50**, 6425–6436.
52 K. E. Erkkila, D. T. Odom and J. K. Barton, *Chem. Rev.*, 1999, **99**, 2777–2796.
53 L.-N. Ji, X.-H. Zou and J.-G. Liu, *Coord. Chem. Rev.*, 2001, **216–217**, 513–536.
54 C. Metcalfe and J. A. Thomas, *Chem. Soc. Rev.*, 2003, **32**, 215–224.
55 S. Shi, J. Zhao, X. Geng, T. Yao, H. Huang, T. Liu, L. Zheng, Z. Li, D. Yang and L. Ji, *Dalton Trans.*, 2010, **39**, 2490–2493.
56 S. Shi, J. Zhao, X. Gao, C. Lv, L. Yang, J. Hao, H. Huang, J. Yao, W. Sun, T. Yao and L. Ji, *Dalton Trans.*, 2012, **41**, 5789–5793.
57 W. Paw and R. Eisenberg, *Inorg. Chem.*, 1997, **36**, 2287–2293.
58 Z. Yang, J. Wang, L. Li, C. Ye and H. Liu, *J. Heterocycl. Chem.*, 2009, **46**, 788–790.
59 J. Bolger, A. Gourdon, E. Ishow and J.-P. Launay, *Inorg. Chem.*, 1996, **35**, 2937–2944.
60 B. P. Sullivan, D. J. Salmon and T. J. Meyer, *Inorg. Chem.*, 1978, **17**, 3334–3341.
61 S. Satyanarayana, J. C. Dabrowiak and J. B. Chaires, *Biochemistry*, 1992, **31**, 9319–9324.
62 Y. Liu, M. Li, Q. Zhao, H. Wu, K. Huang and F. Li, *Inorg. Chem.*, 2011, **50**, 5969–5977.
63 R. Faust and S. Ott, *J. Chem. Soc., Dalton Trans.*, 2002, 1946–1953.
64 P. Murat, Y. Singh and E. Defrancq, *Chem. Soc. Rev.*, 2011, **40**, 5293–5307.
65 M. J. Frisch, G. W. Trucks, H. B. Schlegel, G. E. Scuseria, M. A. Robb, J. R. Cheeseman, J. A. Montgomery, T. Vreven, K. N. Kudin, J. C. Burant, J. M. Millam, S. S. Iyengar, J. Tomasi, V. Barone, B. Mennucci, M. Cossi, G. Scalmani, N. Rega, G. A. Petersson, H. Nakatsuji, M. Hada, M. Ehara, K. Toyota, R. Fukuda, J. Hasegawa, M. Ishida, T. Nakajima, Y. Honda, O. Kitao, H. Nakai, M. Klene, X. Li, J. E. Knox, H. P. Hratchian, J. B. Cross, V. Bakken, C. Adamo, J. Jaramillo, R. Gomperts, R. E. Stratmann, O. Yazyev, A. J. Austin, R. Cammi, C. Pomelli, J. W. Ochterski, P. Y. Ayala, K. Morokuma, G. A. Voth, P. Salvador, J. J. Dannenberg, V. G. Zakrzewski, S. Dapprich, A. D. Daniels, M. C. Strain, O. Farkas, D. K. Malick, A. D. Rabuck, K. Raghavachari, J. B. Foresman, J. V. Ortiz, Q. Cui, A. G. Baboul, S. Clifford, J. Cioslowski, B. B. Stefanov, G. Liu, A. Liashenko, P. Piskorz, I. Komaromi, R. L. Martin, D. J. Fox, T. Keith, A. Laham, C. Y. Peng, A. Nanayakkara, M. Challacombe, P. M. W. Gill, B. Johnson, W. Chen, M. W. Wong, C. Gonzalez and J. A. Pople, 2003.
66 M. K. Nazeeruddin, F. De Angelis, S. Fantacci, A. Selloni, G. Viscardi, P. Liska, S. Ito, B. Takeru and M. Grätzel, *J. Am. Chem. Soc.*, 2005, **127**, 16835–16847.
67 C. Barolo, M. K. Nazeeruddin, S. Fantacci, D. Di Censo, P. Comte, P. Liska, G. Viscardi, P. Quagliotto, F. De Angelis, S. Ito and M. Grätzel, *Inorg. Chem.*, 2006, **45**, 4642–4653.
68 P. Gąsiorski, K. S. Danel, M. Matusiewicz, T. Uchacz and A. V. Kityk, *Dyes Pigm.*, 2012, **93**, 1538–1543.
69 C. Lee, W. Yang and R. G. Parr, *Phys. Rev. B*, 1988, **37**, 785–789.
70 A. D. Becke, *Phys. Rev. A: At., Mol., Opt. Phys.*, 1988, **38**, 3098–3100.
71 A. D. Becke, *J. Chem. Phys.*, 1993, **98**, 5648–5652.
72 A. Rajendran, C. Zhao, B. Rajendar, V. Thiagarajan, Y. Sato, S. Nishizawa and N. Teramae, *Biochim. Biophys. Acta, Gen. Subj.*, 2010, **1800**, 599–610.
73 W. R. Wadt and P. J. Hay, *J. Chem. Phys.*, 1985, **82**, 284–298.
74 P. J. Hay and W. R. Wadt, *J. Chem. Phys.*, 1985, **82**, 270–283.
75 S. Agrawal, R. P. Ojha and S. Maiti, *J. Phys. Chem. B*, 2008, **112**, 6828–6836.

76 G. M. Morris, R. Huey, W. Lindstrom, M. F. Sanner, R. K. Belew, D. S. Goodsell and A. J. Olson, *J. Comput. Chem.*, 2009, **30**, 2785–2791.
77 O. Trott and A. J. Olson, *J. Comput. Chem.*, 2010, **31**, 455–461.
78 K. Chen, S. J. Adelstein and A. I. Kassis, *THEOCHEM*, 2004, **711**, 49–56.
79 S. Thangapandian, S. John, S. Sakkiah and K. W. Lee, *J. Chem. Inf. Model.*, 2010, **51**, 33–44.
80 P. Ragazzon and J. B. Chaires, *Methods*, 2007, **43**, 313–323.
81 J. Ren and J. B. Chaires, *Biochemistry*, 1999, **38**, 16067–16075.
82 Y. Sun, D. A. Lutterman and C. Turro, *Inorg. Chem.*, 2008, **47**, 6427–6434.
83 S. Masiero, R. Trotta, S. Pieraccini, S. De Tito, R. Perone, A. Randazzo and G. P. Spada, *Org. Biomol. Chem.*, 2010, **8**, 2683–2692.
84 E. M. Rezler, J. Seenisamy, S. Bashyam, M.-Y. Kim, E. White, W. D. Wilson and L. H. Hurley, *J. Am. Chem. Soc.*, 2005, **127**, 9439–9447.
85 S. Shi, X. Geng, J. Zhao, T. Yao, C. Wang, D. Yang, L. Zheng and L. Ji, *Biochimie*, 2010, **92**, 370–377.
86 V. Đapić, V. Abdomerović, R. Marrington, J. Peberdy, A. Rodger, J. O. Trent and P. J. Bates, *Nucleic Acids Res.*, 2003, **31**, 2097–2107.
87 P. Wu, D.-L. Ma, C.-H. Leung, S.-C. Yan, N. Zhu, R. Abagyan and C.-M. Che, *Chem.–Eur. J.*, 2009, **15**, 13008–13021.
88 D. Monchaud and M.-P. Teulade-Fichou, *Org. Biomol. Chem.*, 2008, **6**, 627–636.
89 T.-m. Ou, Y.-j. Lu, J.-h. Tan, Z.-s. Huang, K.-Y. Wong and L.-q. Gu, *ChemMedChem*, 2008, **3**, 690–713.